



Fiber entanglements as a proxy for anthropogenic pollution uptake: Monitoring deep-water rose shrimp (*Parapenaeus longirostris*) throughout the year[☆]

María Ariadna Redón-Morte ^a , Ester Carreras-Colom ^{a,*} , Lorenzo Chiacchio ^b , Alessandro Cau ^b , Oriol Rodríguez-Romeu ^a , Anna Soler-Membrives ^a

^a Departament de Biologia Animal, Biologia Vegetal i Ecologia, Universitat Autònoma de Barcelona, Cerdanyola del Vallès, 08193, Barcelona, Spain

^b Dipartimento di Scienze della Vita e dell'Ambiente, Università degli Studi di Cagliari, Via Tommaso Fiorelli 1, 09126, Cagliari, Italy

ARTICLE INFO

Keywords:

Plastic pollution
Microplastics
Fibers
Crustacea
Health condition
Bioindicator

ABSTRACT

Anthropogenic pollution is considered one of the most concerning threats to marine wildlife and several studies have highlighted that decapod crustaceans might be amongst the most impacted organisms. However, limited attention has been given to the deep-water rose shrimp (*Parapenaeus longirostris*), a Mediterranean crustacean with great ecological and commercial value, especially in the westernmost areas of its distribution. This study analyses variations in anthropogenic fibers (AFs) ingestion in *P. longirostris* throughout the year, as well as potential effects on their health status in the northwestern Mediterranean Sea. Individuals were collected during eight months over the course of a year at depths of 200–500m off the coast of Barcelona. Digestive contents were visually examined to detect the presence of isolated and entangled fibers, which were further characterized using optical microscopy and FTIR spectroscopy. Over 80 % of individuals had ingested AFs with an average abundance of 3.08 fibers per individual. Tangled fibers were also common (~50 %) and reached mean values around 2 mm in diameter. Differences throughout the year were observed in the polymer composition of fibers and the prevalence of entanglements. Additionally, the relationship between the prevalence and complexity of entanglement and biological traits (reproduction and molting) was discussed. No clear effects of the overall occurrence of AFs on shrimp condition were observed. Nonetheless, the findings point out that these decapods are among the marine faunal groups with the highest AF uptake. Fiber entanglements provide a longer temporal integration window for monitoring plastic pollution compared to other commonly used groups (e.g., fish). Thus, using fiber entanglements as a proxy for anthropogenic pollution, combined with the selection of *P. longirostris* as a target species, presents a trustworthy and affordable approach for assessing environmental plastic contamination.

1. Introduction

Every year, between 19 and 23 million metric tonnes of plastic waste enter aquatic ecosystems, highlighting the scale of human-derived pollution in marine environments (Borrelle et al., 2020). This accumulation is particularly concerning because the timescales for the complete degradation of synthetic polymers in the ocean remain unknown, meaning that oceans effectively function as long-term reservoirs for plastic debris (Law, 2017). As a result, plastic pollution has become a widely recognized environmental issue, drawing attention from scientists, policymakers, and the general public (MacLeod et al., 2021)

Among all plastic debris, however, microplastics (MPs) have raised even greater concerns due to their small size as well as their ubiquity and persistence (Bergmann et al., 2017).

MPs are defined as synthetic solid particles ranging from 1 μ m to 1 mm (Hartmann et al., 2019) and represent a highly heterogeneous assemblage, differing in size, shape, and chemical composition, among other characteristics (Hidalgo-Ruz et al., 2012). Notably, fibers have stood out as the most prevalent type detected in the marine environment, leading to increased scientific focus on fiber pollution (Santini et al., 2022). It is worth mentioning that non-digestion-assisted methods seeking MPs in environmental matrices have underscored that an

[☆] This paper has been recommended for acceptance by Charles Wong.

* Corresponding author.

E-mail address: Ester.Carreras.Colom@uab.cat (E. Carreras-Colom).

important fraction of the microlitter present in the environment are fibers of non-synthetic composition (Suaria et al., 2020). As a matter of fact, cellulosic fibers are particularly abundant in the Mediterranean continental shelf and deep seafloor (Sanchez-Vidal et al., 2018) and have been retrieved from the digestive contents of several marine species (Rodríguez-Romeu et al., 2020; Muns-Pujadas et al., 2023; Santon Nicola et al., 2023). Given that cellulosic fibers pose environmental concerns similar to those of synthetic (i.e. plastic) fibers (Ladewig et al., 2015), the term Anthropogenic Fibers (AFs) may more accurately describe this type of marine pollution. This broader term, as defined by Lahens et al. (2018), includes both plastic fibers synthesized from petrochemicals and non-synthetic fibers made from naturally occurring polymers like cellulose, which are still considered artificial.

Regardless of the polymeric composition, microlitter spanning this size range facilitates ingestion by aquatic organisms, particularly those with non-selective feeding strategies or inhabiting the most contaminated sites (Rodríguez-Romeu et al., 2024). Among marine species, benthic crustaceans have been especially recognized for exhibiting higher levels of ingestion and potential accumulation of AFs compared to other organisms, such as fish (Hermsen et al., 2018; Marmara et al., 2023). Moreover, their broad distribution, feeding habits, rapid reproduction and sensitivity to pollutants make them suitable bioindicators of AFs contamination (D'Iglio et al., 2022). In particular, deep-sea decapods such as the red shrimp (*Aristeus antennatus*) and the Norway lobster (*Nephrops norvegicus*) have been highlighted as particularly suitable indicators of microlitter because of their benthic ecological roles and relevance to fisheries (Cau et al., 2019). As research has mainly focused on *N. norvegicus* and *A. antennatus* (Cau et al., 2023; Joyce et al., 2023), other deep-water crustaceans have remained fairly underexplored, particularly in the western Mediterranean. Only a few studies have examined anthropogenic particle ingestion by the deep-water rose shrimp (*Parapenaeus longirostris* Lucas, 1846) in the central and eastern basins (Bono et al., 2020; D'Iglio et al., 2022; Yücel, 2023; Ciaralli et al., 2024). Its benthopelagic lifestyle and allegedly short lifespan (2–3 years) make it an excellent bioindicator for detecting short-term seabed pollution (Yücel, 2023).

In a context of increasing thermal anomalies and progressive warming of deep Mediterranean waters, the selection of suitable bioindicators must consider not only ecological relevance and broad spatial distribution, but also the species' ability to tolerate such changes. A good bioindicator should be easily obtainable, resilient to the monitored stressors, distributed across a wide geographic and bathymetric range, and consistent over time (Bonanno and Orlando-Bonaca, 2018). *P. longirostris*, being both thermophilic and eurythermal, fulfills these criteria, making it a suitable long-term option for monitoring efforts. Moreover, unlike other deep-sea species, its populations appear to thrive with the rising temperatures (Colloca et al., 2014). As a matter of fact, in recent years, an increase in its populations has been observed in the fishing grounds off Barcelona (NW Mediterranean Sea; GSA 6N), where the species is already being commercially exploited (ICATMAR, 2021).

Within the NW Mediterranean Sea, the Barcelona metropolitan area represents the most densely populated urban and industrial area, making it a historically impacted area for various anthropogenic pollutants (Palanques et al., 2008). Previous studies have reported concerning levels of AF ingestion in deep-water decapods, particularly in *A. antennatus*, reaching values over 150 fibers per individual (Carreras-Colom et al., 2020). Additionally, a negative correlation between fiber load and gonadosomatic index (GSI) suggested potential reproductive impairment. However, since this study included only limited sampling opportunities the potential temporal variations associated with reproductive variables may not have been accounted for, and the potential effect on fitness remains unclear to date. Several factors may play a key role in regulating the ingestion, accumulation and egestion of fibers in decapods, including but not limited to the contaminant's characteristics or shrimp's molting processes and feeding strategies (Joyce et al., 2022).

In light of all considerations, the present study aims (1) to characterize AF ingestion levels in *P. longirostris* from the NW Mediterranean Sea, (2) to analyze temporal variations in AF ingestion throughout a year and their relationship with biological factors, and (3) to assess the potential impact of AF ingestion on shrimp's health condition.

2. Materials and methods

2.1. Study area and data collection

A total of 80 adult *Parapenaeus longirostris* individuals, 10 for each temporal sampling, were collected directly from commercial fishing vessels operating nearby Barcelona fishing grounds (Spain, NW Mediterranean Sea) at depths ranging between 189 and 465 m (Fig. 1). The samplings started on February 2022 and were conducted over a year, approximately every two months, with a total of eight samplings (as detailed in Supplementary Material Table S1).

Individuals were frozen at -20°C until analysed. Dissection was conducted within a safety laminar flow cabinet (class II), and the digestive system (stomach and intestine) was removed. For each individual, total body weight (TW), cephalothorax length (CL), hepatopancreas weight (HeW) and gonad weight (GoW) were recorded. Stomach and intestine repletion were visually determined for each individual from 0 % (empty) to 100 % (full) according to the volume of the content.

Furthermore, sex was recorded, and the maturity stage of females was also determined following criteria of Follesa and Carbonara (2019) and Carbonell et al. (2006) with adaptations (Supplementary Material, Table S2).

The hardness of the carapace was assessed to estimate the molting stage as proposed by Milligan et al. (2009) for *Nephrops norvegicus*. Individuals were classified based on whether they had hard or soft carapaces when squeezed between the eyes; those with hard carapaces were considered to be in the intermoult stage, while those with softer ones were categorized as either in the early intermoult or at post-moult stage.

2.2. Characterization of anthropogenic items (AFs)

The digestive systems were screened for the presence of putative AFs using a stereomicroscope (Leica MZ16). AFs were counted and separated as either isolated fibers or entanglements of fibers. Free fibers, defined as those not found entangled to others, are hereafter referred to as isolated fibers.

Isolated fibers were mounted on glass slides with distilled water for further characterization through optical microscopy and images were taken using a ProgRes® C3 (JENOPTIK Optical Systems GmbH, Germany) coupled to a Leica DM500B microscope. The total length of each fiber was determined using AutoCAD (AutoCAD, 2023) software and further classified into three dimensional classes: microfibers ($<1\text{ mm}$), mesofibers ($1\text{--}5\text{ mm}$) and macrofibers ($>5\text{ mm}$). Color was also recorded, recognizing six main categories: transparent, yellowed, red, green, blue and dark tones. Lastly, through optical microscopy, each fiber was assigned a typology based on its features according to predefined criteria (Carreras-Colom et al., 2020). This characterization has proven successful determining the polymer type as every polymer has signature characteristics (Supplementary Material, Table S3). Fibers showing signs of potential biologic origin (i.e., ornamentation, segmentation) were discarded. Subsequently, Fourier-Transformed Infrared Spectrometry (FTIR) was conducted on a randomly selected subsample corresponding to approximately 25 % of the total isolated fibers screened. This selection was weighted based on the relative abundance of fibers in each sampling and visual category, ensuring the inclusion of at least 20 % of the fibers found for each category established. Spectra were captured using an Alpha II FTIR spectrometer in ATR mode (Bruker Optik GmbH, Germany), treated with Spectragraph v1.2.16.1 (Menges, 2021), and compared with reference spectra (see Carreras-Colom et al.,

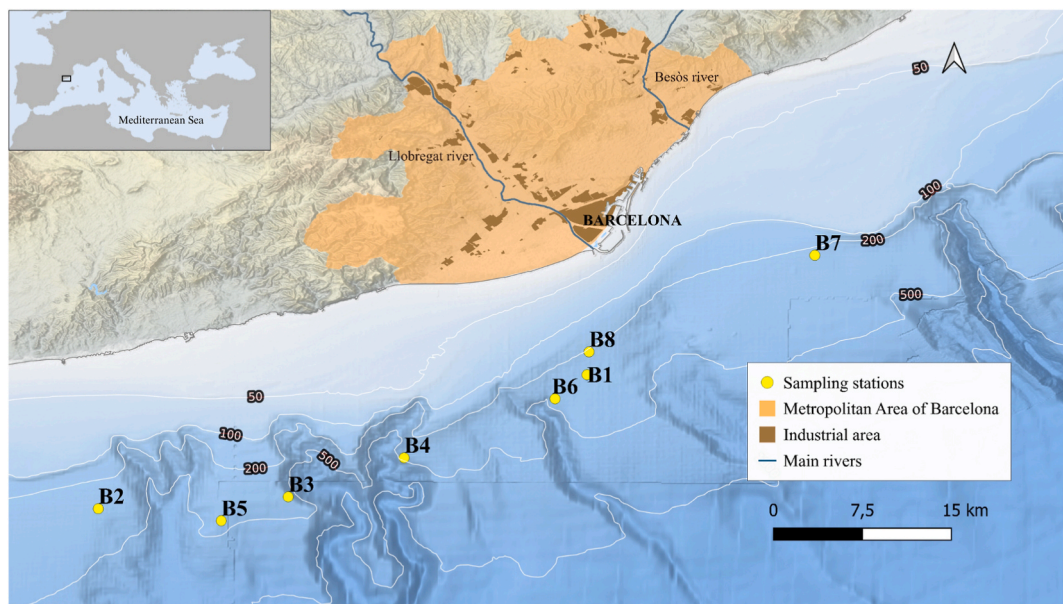


Fig. 1. Map of the study area showing the locations of sampled *Parapenaeus longirostris* individuals analysed for the presence of AFs (yellow dots). Main rivers (Besòs and Llobregat) industrial areas (brown), and the metropolitan area of Barcelona (orange) are also represented. The background map is from EMODnet Bathymetry Consortium (2016): EMODnet Digital Bathymetry (DMT). <https://doi.org/10.12770/c7b53704-999d-4721-b1a3-04ec60c87238>. Land and the industrial areas data reprinted from SIOSE [www.siose.es] under a CC BY licence, original copyright 2016. River data reprinted from [aca.gencat.cat] under a CC BY licence, original copyright 2012. (For interpretation of the references to color in this figure legend, the reader is referred to the Web version of this article.)

2020 for more details on the procedure). The concordance between visually identified typologies and chemically determined polymer compositions exceeded 90 % (Supplementary Material, Fig. S1, Table S3), and thus each fiber was assigned a polymeric composition according to its visually determined typology.

When encountered, entanglements of fibres were photographed, measured (mean diameter, MD, in mm), and categorized according to their morphology and size following the criteria proposed by Carreras-Colom et al. (2020) for *Aristeus antennatus*. Briefly, four dimensional classes of increasing size complexity were determined (B-I to B-IV). Afterwards, a subsample of entanglements (~20 %) from each category (I-IV) was untangled and characterized following the same procedure as for isolated fibers. This process aimed to ensure that the estimates of fiber length and number of fibers per entanglement according to their complexity were consistent with the criteria used to define the categories. Results from this validation are available in the Supplementary Material (Table S4).

2.3. Quality assurance and quality control (QA/QC)

Procedures to minimize the risk of contamination, following those described in Carreras-Colom et al. (2020), included rinsing all equipment with filtered water (200 μ m) and checking it prior to use, wearing cotton lab coats and nitrile gloves, and covering the working area, including the stereomicroscope, with an isolation device. Air controls were conducted to assess the device's efficiency in minimizing airborne contamination and deposition rates.

2.4. Data analysis

Prevalence of fibers (PvF) and entanglements (PvE) was calculated for each sampling point as the percentage of individuals with at least one isolated fiber or entanglement, respectively. Fiber load was also assessed for each individual and organ (i.e. stomach, intestine) in terms of isolated fiber abundance (FN, number of isolated fibers), fiber length (FL, sum of the lengths of all isolated fibers) and estimated total length (TL, sum of FL and the estimated total length of entangled fibers). When

measured values were available from a subsample of untangled entanglements, these were used; for the rest, estimated lengths were assigned based on the entanglement category using averages from the subsample, and included in TL calculations. Statistical differences were assessed using the Kruskal-Wallis test and, when appropriate, the Mann-Whitney *U* test. Temporal differences in the presence of AFs and PvE were explored by means of a generalized linear model (GLM) with a binomial family distribution. Analysis of fiber load (FN, FL, TL) involved Kruskal-Wallis tests coupled with Dunn's post-hoc (*dunn.test* package; Dinno, 2024), as the criteria for normality and homoscedasticity, required for parametric analysis, were not met. Furthermore, temporal differences in the polymer composition of fibers were explored through Permutational Analysis Of Variance (PERMANOVA) on the Bray-Curtis distance-based resemblance matrices of square-root transformed data (*vegan* package; Oksanen et al., 2022).

Differences in the mean size of fibers for each polymer type were analysed using Kruskal-Wallis tests coupled with Dunn's post-hoc tests. Additionally, differences in the fiber size distribution of each polymer were further examined by comparing the histograms of size frequencies. This comparison involved calculating the Kolmogorov-Smirnov (KS) distance and testing for differences using bootstrapping (*Matching* package; Sekhon, 2011).

GLMs fitted with a binomial distribution (*stats* package; R Core Team, 2023), were used to analyze the association between biological variables (CL, sex, carapace hardness), temporal variability (associated to sampling), and the prevalence of fibers and entanglements (PvF, PvE). Similarly, GLM with negative binomial and Tweedie distributions or LM were used to test similar associations with fiber load descriptors (FN, FL, TL) and the entanglements diameter respectively, as response variables. A stepwise selection procedure based on permutational tests was used to select the most explanatory variables.

Shrimp's condition was determined by the relative condition factor ($Kn = W/EW$, where EW is the expected weight from the weight-length regression adjusted with all individuals sampled in the study), hepatosomatic index ($HSI = HeW/TW * 100$) and gonadosomatic index (only in females, $GSI = GoW/TW * 100$). Moreover, Spearman's correlation between and among AFs descriptors (FN, FL, TL) and condition

indices were also calculated.

Finally, a Principal Component Analysis (PCA) was performed using a set of biological variables (CL, Kn, HSI, GSI) and AF descriptors (presence of fibers and entanglements, FN and FL), to visualize potential patterns and relationships. All statistical analyses were performed using R software, version 4.2.3 (R Core Team, 2023). Significance levels were fixed at 0.05 for each statistical hypothesis test.

3. Results

3.1. Characterization of AF ingestion

All *Parapenaeus longirostris* individuals were adults, comprising 36 % males and 64 % females, with sizes (CL) ranging between 21.16 - 31.26 mm and 22.79–36.44 mm, respectively (Supplementary Material, Table S5). Across individuals, the digestive system was generally found to be full, with more than 50 % exhibiting repletion levels of 70 % or higher.

From the total of individuals screened, 67 (83.8 %) were found to contain at least one fiber or entanglement of fibers, with an average of 4.34 ± 3.43 fibers per individual. No fragments or items with other shapes were present. AFs consisted primarily of isolated fibers (a total of 257), measuring between 0.4 and 15.6 mm. Nearly all of them measured over 1 mm (93.8 %), with meso-sized fibers (1–5 mm) accounting for 66.4 % of the total. Macro-sized fibers (>5 mm) were less abundant, representing 27.6 %. Those fibers were detected throughout the digestive system, with a higher prevalence and fiber load in the stomach (PvF = 66.2 %; FL = 13.27 ± 14.33 mm·individual $^{-1}$) compared to the intestines (PvF = 31.2 %; FL = 1.89 ± 3.42 mm·individual $^{-1}$) (Mann-Whitney U test, W = 4803.5, $p < 0.001$, one-sided test). Over 48.8 % of shrimps contained entanglements of fibers, which were found in the stomach in 92.3 % of cases, with diameters ranging between 0.9 and 4.5 mm (Fig. 2). The most frequent entanglements were those categorized as B-III (30.8 %), followed by B-IV (28.2 %), B-II (23.1 %), and B-I (17.9 %).

Once the correspondence between visual typologies and polymer compositions was applied (Supplementary Material, Table S3), the polymer composition of fibers, in decreasing order of abundance, were polyethylene terephthalate (PET), acrylic, cellulosic, polyamide, polyethylene and polypropylene (Fig. 3A; Supplementary Material, Fig. 1). Isolated fibers exhibited a wide range of colors, with transparent fibers being the most abundant (29.8 %), followed by blues (24.6 %), yellowed (28.0 %), red (8.8 %), dark tones (5.3 %), and green (3.5 %).

Significant differences were observed in the mean size of fibers depending on their polymeric composition (KW: $X^2 = 20.736$, df = 6, $p = 0.002$). Specifically, cellulosic fibers were found to be shorter than PET ($p = 0.001$) and polyamide ($p = 0.0178$) fibers (Fig. 3B). Significant differences in the size distribution were also found with cellulosic fibers showing a skewed distribution towards smaller sizes in comparison to PET (KS: D = 0.4, $p = 0.0004$), polyamide (KS: D = 0.456, $p = 0.007$) and acrylic (KS: D = 0.322, $p = 0.025$) fibers (Fig. 3B).

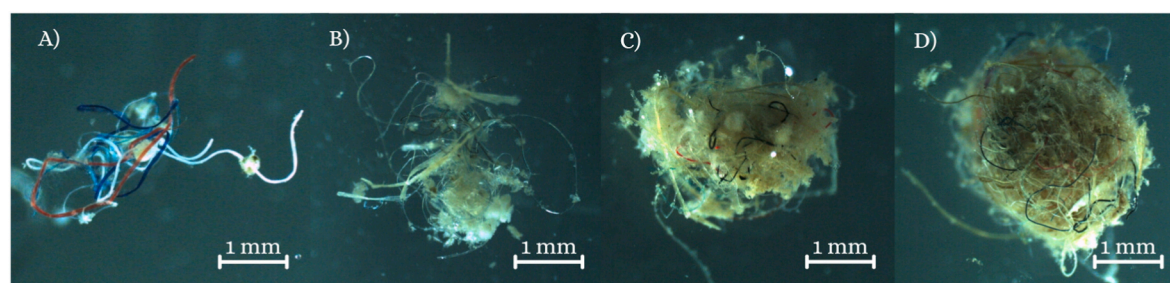


Fig. 2. Entangled balls of fibers with increasing level of complexity. (A) Category B-I: aggregations of fibers in very loose entanglements; (B) Category B-II: loose entanglements with recognizable core, (C) Category B-III: tight entanglements with tight identifiable core, (D) Category B-IV: tight entanglements with several complex core structures. See Supplementary Material Table S4 for more details on the classification.

3.2. Temporal variations in AF ingestion

Overall, at least 60 % of the shrimps from each sampling point contained AFs, either isolated or entangled. In terms of prevalence, significant differences in entanglements (PvE) were observed among temporal samplings (Binomial GLM; $p = 0.003$). Individuals from March and September showed an absence of entanglements, while higher prevalences (>60 % of the individuals) were found in May and November 2022 and February 2023.

Isolated fiber load descriptors (FN, FL) did not significantly vary throughout the year (KW; $p > 0.05$) although mean values of FN in February and November 2022 were approximately twice the values of the other samplings (Table 1). The total estimated length (TL) showed temporal variations (KW: $X^2 = 26.053$, df = 7, $p < 0.001$) with the greatest values being estimated in shrimps from May and November 2022 (Table 1).

Multivariate analysis also showed significant differences among sampled months on polymer composition (PERMANOVA; $p = 0.006$). PET was the most predominant polymer identified in six out of eight samplings locations, accounting for more than >40 % of all fibers found (Supplementary Material, Table S6). The greatest variations to this pattern were observed in individuals sampled in July and September 2022, where PET accounted for 11.1 % and 19.2 % of the total fiber load, respectively. In these sampling locations, the proportion of polyethylene was higher (~23–30 %), compared to less than 5.0 % in the other samples (Supplementary Material, Table S6).

Regarding the size and complexity of the entanglements, no significant temporal differences were found (LM; $F_{5,33} = 0.308$; $p > 0.05$). However, it is worth noting that in May, a notable proportion of B-IV (present in 60 % of the individuals), representing the most complex entanglements, was observed, whereas in March and September, none of the shrimps analysed contained entanglements, neither simple nor complex (Fig. 4A and B).

3.3. Relationship of AF ingestion with biological variables and shrimp's condition

Two distinct peaks of maturity in females were identified: one in March 2022 and another in January 2023, the latter characterized by 100 % of the identified females being in stage IV maturity (Fig. 4C). In contrast, soft carapaces were exclusively observed in July and September 2022, and January 2023 (Fig. 4D).

No strong significant correlations ($p < 0.33$) were found between fiber load descriptors (FN, FL, TL) and the condition indices (Kn, HSI, GSI), while fiber load descriptors were highly correlated with each other ($p > 0.9$). Further analysis of the association between fiber load descriptors (FN, FL) and biological and temporal variables revealed some significant relationships. Carapace hardness was identified as the most relevant predictor for both FN and FL, with individuals with soft carapaces showing significantly lower fiber loads both in terms of abundance and total length (Negative Binomial GLM; $z = -2.39$, $p = 0.017$, and

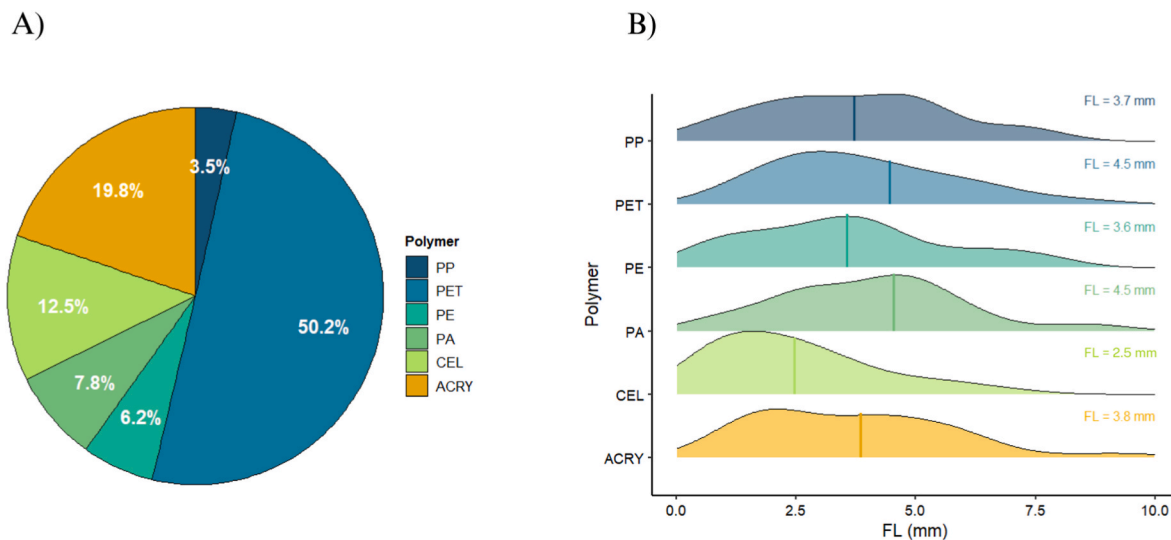


Fig. 3. (A) Polymer composition of all fibers identified from *Parapenaeus longirostris* sampled. (B) Fiber size (FL, mm) by polymer type distribution. Acronyms used: acrylic (ACRY), cellulosic (CEL), polyamide (PA), polyethylene (PE), polyethylene terephthalate (PET), and polypropylene (PP).

Table 1

Mean values (standard deviation) of fiber load descriptors: isolated fiber abundance per individual (FN), total fiber length of isolated fibers (FL) and total length of fibers including isolated and entangled estimate (TL) in digestive contents of *Parapenaeus longirostris* sampled in eight months over a year 2022–2023. Mean values of relative contribution to the total load of fibers in percentage is noted following mean values (SD). For details on samplings performed see [Supplementary Material Table S1](#).

Sampling	FN		FL		TL	
	n-ind ⁻¹ (SD)	%	mm-ind ⁻¹ (SD)	%	mm-ind ⁻¹ (SD)	%
February 2022	4.20 (5.77)	16.9	24.1 (28.8)	23.5	45.5 (52.0)	6.0
March 2022	2.2 (2.66)	8.9	8.54 (9.13)	8.3	8.54 (9.13)	1.1
May 2022	3.10 (3.75)	12.5	9.53 (10.1)	9.3	228 (187)	30.3
July 2022	2.7 (1.34)	10.9	9.83 (7.20)	9.4	89.7 (120)	11.9
September 2022	2.6 (3.41)	10.5	10.6 (14.2)	10.3	10.7 (14.2)	1.4
November 2022	4.6 (3.92)	18.5	19.2 (11.6)	18.7	198 (159)	26.3
January 2022	2.00 (2.21)	8.9	7.00 (9.84)	6.8	69.4 (115)	9.2
February 2023	3.2 (1.81)	12.9	14.2 (8.72)	13.7	103 (114)	13.7

Tweedie GLM; $t = -2.85$, $p = 0.0056$, for FN and FL, respectively).

No significant effects of CL or condition indices were observed over fiber load descriptors (GLM, $p > 0.05$).

The Principal Component Analysis (PCA) revealed that the first two components captured over 50 % of the total variance, effectively summarizing the data (Supplementary Material, Fig. S2). The first principal component (PC1, 34.3 %) was positively correlated with FN and TL variable, and to a lesser extent with the presence of fibers and entanglements. Individuals positioned on the right side of the PCA plot exhibited higher TL and FN values, particularly in February, September, and November 2022, coinciding with a greater occurrence of entanglements. The second component (PC2, 18.25 %) was associated with HSI and CL, showing that individuals from May and July presented higher CL and lower HSI values, whereas those from February and November 2022, January 2022, and February 2023 displayed the opposite trend. Overall, individuals showed broad dispersion across sampling points, suggesting a great within-group variability.

4. Discussion

This study is the first to assess the prevalence, abundance and characteristics of AFs, mainly plastic fibers, ingested by the deep-sea shrimp *P. longirostris* in the northwestern Mediterranean Sea over an extended period. Fiber ingestion was reported in every sampling throughout 2022–2023, demonstrating the pervasive nature of marine debris on the Barcelona coast.

4.1. Prevalence and abundance of AF in *Parapenaeus longirostris*

The first record of debris in *P. longirostris* was by [Bono et al. \(2020\)](#) in the Strait of Sicily (Central Mediterranean), with fibers and entanglements found in 21 % of individuals. Subsequent studies documented a higher prevalence of AFs and fragments in the Ionian (76 % and 100 %; [D'Iglio et al., 2022](#); [Yücel, 2023](#)) and Tyrrhenian Seas (38 %; [Ciaralli et al., 2024](#)), while the western basin remained relatively unexplored. All studies reported a dominance of fibers or fibrous forms (>75 %, 0.11–10.4 mm) with fragments rarely exceeding 5 %. Fiber entanglements varied, being absent, or at least not explicitly mentioned, in the southwestern Ionian ([D'Iglio et al., 2022](#)), scarce in the Tyrrhenian ([Ciaralli et al., 2024](#)), and abundant in the eastern Mediterranean ([Yücel, 2023](#)). The absolute dominance of AFs either as isolated fibers (85.6 %) and entangled bundles of fibers (14.4 %), with no other shaped objects present at all is consistent with previous studies that demonstrated a clear predominance of fibers over fragments not only in this species ([D'Iglio et al., 2022](#); [Yücel, 2023](#); [Ciaralli et al., 2024](#)) but also in other crustacean species ([Devriese et al., 2015](#); [Carreras-Colom et al., 2018, 2020; 2022a](#); [Chiacchio et al., 2025](#)), supporting that fiber-shaped items are more easily ingested and retained ([Welden and Cowie, 2016a](#)). Furthermore, as suggested by [Avio et al. \(2020\)](#), fibers may also be more common along densely populated coastlines, such as our study area, due to their potential textile origin.

In most existing studies, the extraction of anthropogenic debris involved the chemical digestion of the stomach and intestine, likely eliminating cellulosic fibers and limiting direct comparisons. Despite this, fiber ingestion in the NW Mediterranean Sea appears consistent with levels reported in previous work, which are globally high compared to other Mediterranean regions.

In our study area, notable levels of AFs ingestion have already been reported in other deep-water decapods, such as *A. antennatus* and *N. norvegicus*. Over 75.0 % of *A. antennatus* contained at least one fiber, with some specimens accumulating total fiber lengths of up to 150 mm,

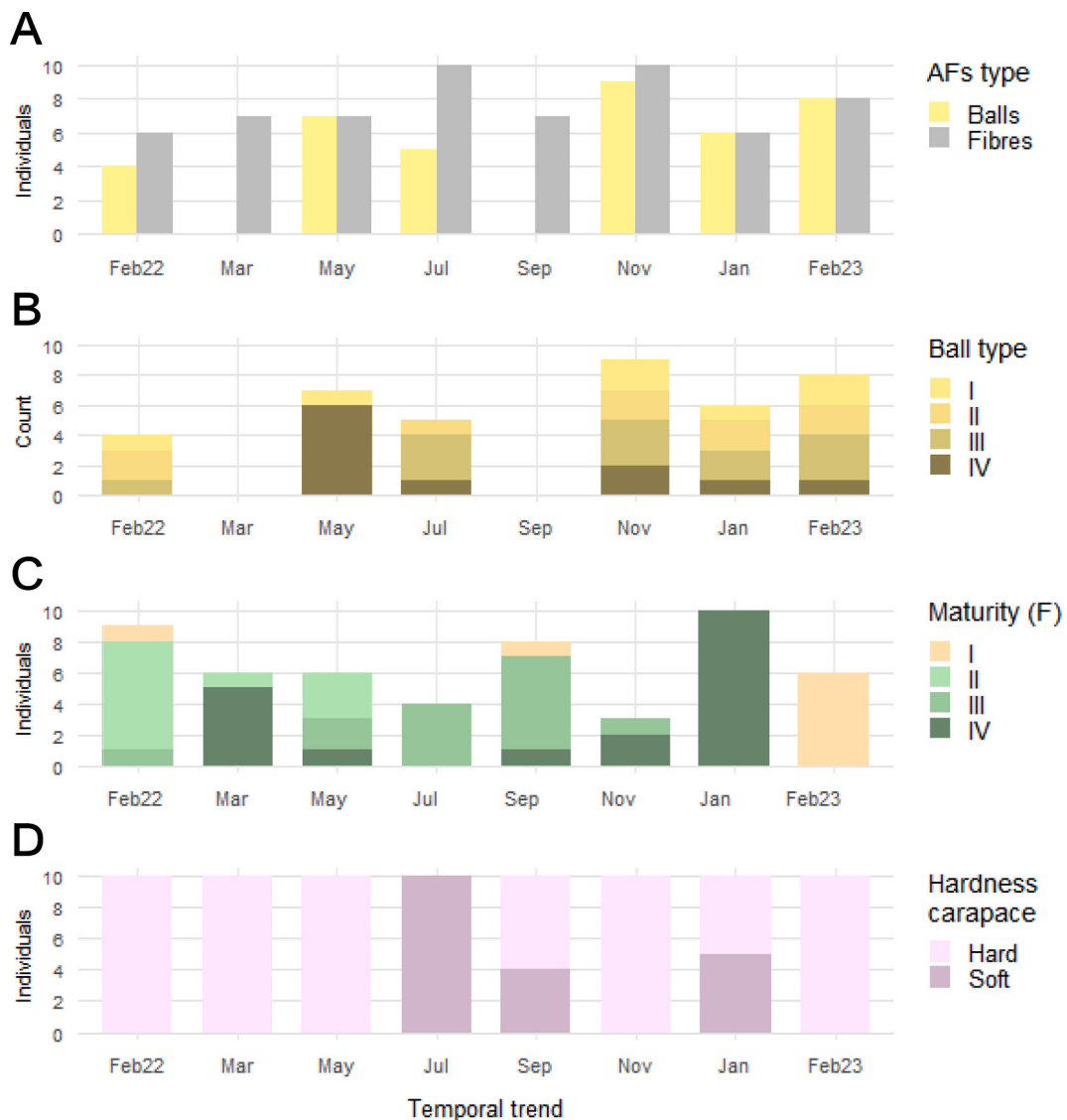


Fig. 4. Temporal trends in (A) prevalence of isolated fibers and entanglements, (B) abundance and complexity of entanglements (C) female maturity, and (D) carapace hardness.

a value far exceeding the animal's body length (Carreras-Colom et al., 2020). Similarly, *N. norvegicus* showed synthetic fibers in 85 % of the stomachs analysed, with higher abundances in specimens captured near the urbanized Barcelona area (Carreras-Colom et al., 2022b).

In addition to local variations in AF environmental concentrations, ingestion levels in decapod species are likely shaped by differences in feeding strategies, body morphology, and seafloor affinities, as well as by the route of exposure, whether through direct accidental or active ingestion or trophic transfer, among other factors (Desforges et al., 2015). *P. longirostris* alternates hunting benthopelagic prey (e.g., crustaceans, cephalopods, small fish), and digging for benthic organisms (e.g., polychaetes, echinoderms, bivalves) (Kapiris, 2004). In the latter case, this habit of exploiting benthic organisms that are more closely associated with the bottom has been pointed as one of the major reasons for the increased levels of AF ingestion observed in other decapods as AFs are expected to accumulate in superficial sediments (Uddin et al., 2021). Moreover, a highly diversified diet and high fullness index values, which altogether mean a high number of ingestion opportunities, would further support a high AF ingestion level in the deep-water rose shrimp, as suggested with the closely related *A. antennatus*, another highly motile and active predator (Cartes, 1994; Chiacchio et al., 2025).

4.2. Polymer and ball characterization

Studies on polymer distribution in the marine environment reveal varying patterns, influenced by polymer density, habitat, and proximity to sources. Lower density polymers (i.e. polypropylene and polyethylene) dominate sea surface areas, whereas denser ones (i.e. polyesters and acrylics) are common at greater depths (Erni-Cassola et al., 2019). This aligns with the two most prevalent polymers found in our study, PET and acrylic (50 and 20 %, respectively). Proximity to highly urbanized areas, such as the Barcelona metropolitan zone, where wastewater overflow has been previously highlighted (Carreras-Colom et al., 2020), supports textile fiber dominance.

Even more notably, cellulosic fibers were the third most abundant polymer (12.5 %), while studies on *A. antennatus* and *N. norvegicus* found only 5 % and 2–3 %, respectively (Carreras-Colom et al., 2020, 2022b). Those studies, included both isolated and entangled fibers, whereas in our study, the polymer composition description was based solely on isolated fibers. Differences between isolated and entangled fibers were not specifically reported in those studies, however unpublished data suggest over 80 % of synthetic fibers (mainly PET) formed the entanglements, due to their greater length and higher resistance to action gastric mill action, thus making them more prone to tangling up. On the

contrary, cellulosic-like fibers might break down due to the gastric mill grinding action and pass through to the intestine. Consequently, isolated fibers better represent ingested AFs and the surrounding environment.

Nonetheless, beyond methodological differences, discrepancies in cellulose prevalence may also reflect ecological differences between the species studied. *Parapenaeus longirostris*, for instance, is most abundant at shallower depths (300–400 m), closer to coastal areas where AFs inputs are typically higher. In contrast, *A. antennatus* occurs at deeper depths (600–1200 m; [Cartes et al., 2017](#)) often associated with submarine canyons ([Cartes, 1994](#)), where cellulosic fibers may degrade more rapidly than synthetic materials ([Pasterk et al., 2024](#)). These conditions, including sources and differential persistence, may explain higher cellulose presence on the continental shelf, where it would remain better preserved, and ultimately ingested by *P. longirostris* in a higher proportion.

Entangled balls of fibers were notably abundant (~50 % of sampled shrimps), measuring between 0.9 and 4.5 mm in diameter. Their formation likely relates to the morphology and functioning of the crustacean digestive system (i.e., gastric mill), which mixes rather than breaks fibers ([Welden and Cowie, 2016a](#)). Interestingly, these bundles often incorporated carbon-based fibers (e.g., plant fibrous remains) and hard fragments (e.g., crustacean carapaces, bivalve shells), making up roughly 30 % of their mass. The abundance of these materials suggests they may act as nucleation centers, facilitating the aggregation of fibers into entangled structures.

Three individuals were found with entanglements in the intestine, something that had never been accounted for so far in other decapods, likely due to the narrow passage from the pyloric stomach to the intestine ([Welden and Cowie, 2016b](#)). Notably, these intestinal entanglements were simpler, one Type II and two Type I, and small enough to bypass the gastric mill and continue through the digestive tract.

4.3. Temporal variations throughout the year

Great effort has been made to characterize plastic ingestion in decapods across the NW Mediterranean Sea, revealing spatial patterns and potential AF pollution hotspots. Notably, studies on *A. antennatus* ([Cartes, 1994](#); [Cartes et al., 2008](#); [Carreras-Colom et al., 2018, 2020](#)) have spanned several decades, offering a long-term perspective on the issue. However, all these efforts relied on sporadic samplings, often based on a single collection per year or over a few months. This made possible inferences on temporal trends almost impossible, keeping a strong suspicion that biology (i.e., feeding, molting, reproduction) of the species would play a key role. Our study addressed this gap by analyzing *P. longirostris* AF ingestion patterns over an entire year.

Accordingly, it was possible to record how the prevalence of entanglements varied significantly over time, with certain months showing no occurrence in any of the sampled individuals, while others (i.e., May and November 2022, and February 2023) demonstrated a high prevalence (>70 %). Similarly, significant temporal differences in fiber load analysis were observed only when both isolated and entangled fibers (i.e., the estimated total load) were considered, highlighting the importance of study timing as a crucial factor for future research.

The prevalence and complexity of entanglements in *P. longirostris* could be linked to the species' feeding, molting, and reproductive dynamics. For instance, in May, complex entanglements (Type IV) were most prevalent, peaking just before shrimps were identified with soft carapaces, in July. By that time, both the frequency and complexity of entanglements declined significantly, and by September, no entanglements were observed. Interpreting carapace softness as the proximity to molting, this observation suggests that the decrease in the presence of entanglements could be linked to some extent to the molting process as proposed by [Welden and Cowie \(2016b\)](#). During molting, crustaceans shed the foregut, where entanglements are commonly trapped, thus facilitating their removal. As shrimps resume feeding post-molting, they would be expected to accumulate fibers again, progressively forming

new entanglements. This cycle would be particularly evident in autumn, when feeding intensity increases to meet energetic demands for winter, raising entanglement prevalence and complexity ([Kapiris, 2004](#); [Sobrino et al., 2005](#)). Moreover, not only is the feeding activity higher in this period, but it has also been related in the Ionian Sea to more intense rooting behavior targeting buried prey ([Kapiris, 2004](#)). Dietary shifts to meet pre-productive energy demands are common in the western basin, though not yet described for this species ([Cartes et al., 2008](#)), and likely increase opportunities for fiber uptake. In a similar way, the high fullness reported throughout spring would support the peak of entanglements of May.

It is important to note that fiber entanglements remained prevalent not only throughout autumn but also well into February of the following year despite molting events during September and January, possibly because only a portion of the individuals had experienced molting or because molting might not completely remove accumulated fibers and entanglements, with less complex entanglements remaining. As a matter of fact, some parts of the gastric mill may be unaffected by molting, with species-specific variation ([Sheridan et al., 2016](#)). Finally, it is possible that fiber re-accumulation in shrimps occurred exceptionally quickly after molting in relation to the remaining entanglements (i.e., the ones already accumulated and not lost during molting) due to an intense phase of feeding and an increased environmental concentration of AFs. Such increased availability has been associated with the region's regime in other studies, with characteristic seasonal storms that often result in flash floods ([Tubau et al., 2015](#)) being hypothesized to release high amounts of fibers into the environment ([Carreras-Colom et al., 2020](#)). In any case, each of these possibilities highlights the need for further targeted research on fiber and entanglement retention across molting events in decapod crustaceans.

Gut blockage and false satiation are common effects of debris ingestion ([Cole et al., 2013](#); [Welden and Cowie, 2016a](#)), but were not observed in the deep-water rose shrimp, which exhibited full intestines at the time of capture, even when entanglements were present. Moreover, the overall fullness index remained high across samples, aligning with what would be expected in penaeid species in the area ([Cartes, 1995](#)), and indicating unaffected feeding activity.

Furthermore, the assessment of shrimp health through condition indices did not suggest any discernible impact attributable to fiber ingestion, with temporal trends fitting those expected according to the reproductive patterns of the species. Although maturing females were found almost all year round (stages III and IV), two clear peaks were detected in spring and early winter which matched GSI variability. These findings are partially consistent with what has been previously reported in the Mediterranean Sea, as there are some discrepancies as when the peaks of maturity occur depending on the geographical area ([Sobrino et al., 2005](#); [Guíjarro et al., 2009](#); [Kasalica et al., 2011](#)). Accordingly, HSI and Kn values peaked during high fullness and before gonad development, a pattern seen in other deep-sea decapods ([Cartes et al., 2008](#); [Fanelli and Cartes, 2008](#)).

4.4. *Parapenaeus longirostris* for monitoring deep-sea environments

It is widely recognized that the unique ecological and biological characteristics of decapods make them particularly susceptible to AF ingestion, rendering them promising bioindicators. Their feeding behavior promotes a close interaction with the sediment-water interface and resuspended sediments, where AFs tend to accumulate ([Woodall et al., 2015](#); [Uddin et al., 2021](#)). Moreover, their biology, particularly the structure of the gastric mill, allegedly facilitates the prolonged retention of fibers, restricting their passage to the intestine and promoting the formation of entanglements or bundles ([Welden and Cowie, 2016a, 2016b](#)) as discussed above. Previous studies found entanglements, also commonly referred to as balls, a more efficient and trustworthy proxy for comparing plastic ingestion among populations of *N. norvegicus* than fiber abundance ([Carreras-Colom et al., 2020](#)).

Furthermore, employing a straightforward visual inspection protocol for detecting these entanglements in digestive contents could greatly reduce contamination risks, avoiding specialized equipment or trained technicians, thereby lowering both costs and time requirements (Lusher and Hernandez-Milian, 2018) while enhancing result reliability.

Our results suggest that relying solely on isolated fibers could greatly underestimate the potential impact of AFs. This underscores the value of using entanglements as a proxy for assessing AF impact in crustaceans during monitoring efforts. At the same time, the assessment of entanglements integrates a broader time window compared to AF ingestion in fish, in which the transit of AFs through the gastrointestinal tract is completed in a matter of hours (Rodríguez-Romeu et al., 2024). Nonetheless, for that purpose, a comprehensive knowledge of the molting dynamics is key to properly adjusting the monitoring temporal samplings. In the case of *P. longirostris*, autumn could be considered an optimal season for carrying such an assessment as, although it was not the period with the greatest impact, it was the one in which more homogeneous results were observed over a considerable time window. Moreover, it is when the species' biology appears to most favor the accumulation of entanglements, which suggests that this pattern would likely be repeated in subsequent years.

All these considerations are applicable to other well studied decapod species inhabiting the Mediterranean Sea, namely *A. antennatus*, *A. foliacea*, *N. norvegicus*. However, *P. longirostris*, together with *A. antennatus*, appears to exhibit the highest levels of fiber ingestion, making them particularly relevant for the study of AF pollution. Unlike *A. antennatus*, *P. longirostris* displays a broader geographic distribution, facilitating regional comparisons. Moreover, being a thermophilic species, its abundance is expected to increase in the coming years, in contrast to species such as *A. antennatus* or *A. foliacea*, whose catches in the Mediterranean have shown high interannual variability. Additionally, the deep-water rose shrimp inhabits depths between 100 and 300 m, a transitional zone of ecological interest and one frequently targeted by fishing fleets, thus making sample collection relatively accessible. Based on all the considerations above, *P. longirostris* emerges as the most suitable target species as bioindicator of plastic pollution, meeting most of the established criteria for effective sentinel species (Fossi et al., 2018).

5. Conclusions

This study provides the first year-round assessment of AF ingestion in *Parapenaeus longirostris*, revealing fibers in over 80 % of individuals and complex entanglements in nearly 50 % of the cases. Temporal patterns were evident when considering both isolated and entangled fibers, highlighting the need to include entanglements in monitoring protocols. Their prevalence and complexity of fiber entanglements showed apparent links with biological cycles, especially molting and feeding intensity, which are eventually related to the reproductive dynamics. Specifically, a decline in the number of individuals retaining fiber entanglements was associated with a peak in molting activity, suggesting that molting may act as a fiber removal mechanism, though not entirely. More research is needed to properly understand the role of molting in the removal of accumulated fibers, as the possibility of removal being incomplete would imply a gradual accumulation of fibers over time that could eventually compromise the organism's condition. Fortunately, shrimp health, evaluated through condition indices, showed no adverse effects.

Altogether, these findings highlight *P. longirostris* as a suitable candidate species for monitoring AF ingestion in the Mediterranean Sea while also providing a baseline to address potential risks of AFs to crustacean species. Further research should explore long-term trends and expand spatial coverage to better understand regional impacts.

CRediT authorship contribution statement

María Ariadna Redón-Morte: Writing – review & editing, Writing – original draft, Investigation, Formal analysis, Data curation. **Ester Carreras-Colom:** Writing – review & editing, Writing – original draft, Methodology, Investigation, Conceptualization. **Lorenzo Chiacchio:** Writing – review & editing, Investigation, Data curation. **Alessandro Cau:** Writing – review & editing, Methodology, Conceptualization. **Oriol Rodríguez-Romeu:** Writing – review & editing, Methodology, Conceptualization. **Anna Soler-Membrives:** Writing – review & editing, Methodology, Funding acquisition, Conceptualization.

Funding

This study was supported by the GARRAF_ENMAR project. This project is developed with the collaboration of the Biodiversity Foundation of the Ministry for Ecological Transition and the Demographic Challenge, through the Pleamar Programme, and is co-financed by the European Union through the European Maritime, Fisheries and Aquaculture Fund. E.C-C. acknowledges financial support from the European Union NextGenerationEU programme.

Declaration of competing interest

The authors declare that they have no known competing financial interests or personal relationships that could have appeared to influence the work reported in this paper.

Acknowledgements

The authors would like to thank the crew of commercial fishing vessels from Barcelona and Vilanova i la Geltrú involved in the present work.

Appendix A. Supplementary data

Supplementary data to this article can be found online at <https://doi.org/10.1016/j.envpol.2025.127337>.

Data availability

Data will be made available on request.

References

- AutoCAD, 2023. Autodesk, Inc. v.1.6 [software], version 1.6). <http://usa.autodesk.com/autocad/>.
- Avio, C.G., Pittura, L., D'Errico, G., Abel, S., Amorello, S., Marino, G., Gorbi, S., Regoli, F., 2020. Distribution and characterization of microplastic particles and textile microfibers in Adriatic food webs: general insights for biomonitoring strategies. Environ. Pollut. 258, 113766. <https://doi.org/10.1016/j.envpol.2019.113766>.
- Bergmann, M., Tekman, M.B., Gutow, L., 2017. Marine litter: sea change for plastic pollution. Nature 544, 297. <https://doi.org/10.1038/544297a>.
- Bonanno, G., Orlando-Bonaca, M., 2018. Perspectives on using marine species as bioindicators of plastic pollution. Mar. Pollut. Bull. 137, 209–221. <https://doi.org/10.1016/j.marpolbul.2018.10.018>.
- Bono, G., Falzone, F., Falco, F., Di Maio, F., Gabriele, M., Gancitano, V., Geraci, M.L., Scannella, D., Mancuso, M., Okpala, C.O.R., Pasti, L., 2020. Microplastics and alien black particles as contaminants of deep-water rose shrimp (*Parapenaeus longirostris* (Lucas, 1846) in the Central Mediterranean Sea. J. Adv. Biotechnol. Bioeng. 8, 23–28. <https://doi.org/10.12970/2311-1755.2020.08.04>.
- Borrelle, S.B., Ringma, J., Law, K.L., Monnahan, C.C., Lebreton, L., McGivern, A., Murphy, E., Jambeck, J., Leonard, G.H., Hilleary, M.A., Eriksen, M., Possingham, H. P., De Frond, H., Gerber, L.R., Polidoro, B., Tahir, A., Bernard, M., Mallos, N., Barnes, M., Rochman, C.M., 2020. Predicted growth in plastic waste exceeds efforts to mitigate plastic pollution. Science 369, 1515–1518. <https://doi.org/10.1126/science.aba3656>.
- Carbonell, A., Grau, A., Laurance, V., Gomez, C., 2006. Ovary development of the red shrimp, *Aristeus antennatus* (Risso, 1816) from the Northwestern Mediterranean Sea. Crustac. Int. J. Crustac. Res. 79, 727–743. <https://doi.org/10.1163/156854006778026807>.

Carreras-Colom, E., Constenla, M., Soler-Membrives, A., Cartes, J.E., Baeza, M., Padrós, F., Carrassón, M., 2018. Spatial occurrence and effects of microplastic ingestion on the deep-water shrimp *Aristeus antennatus*. Mar. Pollut. Bull. 133, 44–52. <https://doi.org/10.1016/j.marpolbul.2018.05.012>.

Carreras-Colom, E., Constenla, M., Soler-Membrives, A., Cartes, J.E., Baeza, M., Carrassón, M., 2020. A closer look at anthropogenic fiber ingestion in *Aristeus antennatus* in the NW Mediterranean Sea: differences among years and locations and impact on health condition. Environ. Pollut. 263, 114567. <https://doi.org/10.1016/j.envpol.2020.114567>.

Carreras-Colom, E., Cartes, J.E., Constenla, M., Welden, N.A., Soler-Membrives, A., Carrassón, M., 2022a. An affordable method for monitoring plastic fiber ingestion in *Nephrops norvegicus* (Linnaeus, 1758) and implementation on wide temporal and geographical scale comparisons. Sci. Total Environ. 810, 152264. <https://doi.org/10.1016/j.scitotenv.2021.152264>.

Carreras-Colom, E., Cartes, J.E., Rodríguez-Romeu, O., Padrós, F., Solé, M., Grelaud, M., Ziveri, P., Palet, C., Soler-Membrives, A., Carrassón, M., 2022b. Anthropogenic pollutants in *Nephrops norvegicus* (Linnaeus, 1758) from the NW Mediterranean Sea: uptake assessment and potential impact on health. Environ. Pollut. 314, 120230. <https://doi.org/10.1016/j.envpol.2022.120230>.

Cartes, J.E., 1994. Influence of depth and season on the diet of the deep-water aristeid *Aristeus antennatus* along the continental slope (400 to 2300 m) in the Catalan Sea (Western Mediterranean). Mar. Biol. 120, 639–648. <https://doi.org/10.1007/BF00350085>.

Cartes, J.E., 1995. Diets of, and trophic resources exploited by, bathyal penaeoidean shrimps from the western mediterranean. Mar. Freshw. Res. 46, 889–996. <https://doi.org/10.1071/MF9950889>.

Cartes, J.E., Papiol, V., Guijarro, B., 2008. The feeding and diet of the deep-sea shrimp *Aristeus antennatus* off the Balearic Islands (Western Mediterranean): influence of environmental factors and relationship with the biological cycle. Prog. Oceanogr. 79, 37–54. <https://doi.org/10.1016/j.pocean.2008.07.003>.

Cartes, J.E., López-Pérez, C., Carbonell, A., 2017. Condition and recruitment of *Aristeus antennatus* at great depths (to 2,300 m) in the Mediterranean: relationship with environmental factors. Fish. Oceanogr. 27, 114–126. <https://doi.org/10.1111/fog.12237>.

Cau, A., Avio, C.G., Dassi, C., Follesa, M.C., Moccia, D., Regoli, F., Pusceddu, A., 2019. Microplastics in the crustaceans *Nephrops norvegicus* and *Aristeus antennatus*: flagship species for deep-sea environments? Environ. Pollut. 255, 113107. <https://doi.org/10.1016/j.envpol.2019.113107>.

Cau, A., Gorule, P.A., Bellodi, A., Carreras-Colom, E., Moccia, D., Pittura, L., Regoli, F., Follesa, M.C., 2023. Comparative microplastic load in two decapod crustaceans *Palinurus elephas* (Fabricius, 1787) and *Nephrops norvegicus* (Linnaeus, 1758). Mar. Pollut. Bull. 191, 114912. <https://doi.org/10.1016/j.marpolbul.2023.114912>.

Chiacchio, L., Cau, A., Soler-Membrives, A., Follesa, M.C., Bellodi, A., Carreras-Colom, E., 2025. Comparative assessment of microplastic ingestion among deep sea decapods: distribution analysis in Sardinian and Catalan waters. Environ. Res. 120962 <https://doi.org/10.1016/j.envres.2025.120962>.

Ciaralli, L., Valente, T., Monfardini, E., Libralato, G., Manfra, L., Berto, D., Rampazzo, F., Gioacchini, G., Chemello, G., Piermarini, R., Silvestri, C., Matiddi, M., 2024. Rose or red, but still under threat: comparing microplastics ingestion between two sympatric marine crustacean species (*Aristaeomorpha foliacea* and *Parapenaeus longirostris*). Animals 14 (15), 2212. <https://doi.org/10.3390/ani14152212>.

Cole, M., Lindeque, P., Fileman, E., Halsband, C., Goodhead, R., Moger, J., Galloway, T., 2013. Microplastic ingestion by zooplankton. Environ. Sci. Technol. 47 (12), 6646–6655. <https://doi.org/10.1021/es400663f>.

Colloca, F., Mastrantonio, G., Lasinio, G.J., Ligas, A., Sartor, P., 2014. *Parapenaeus longirostris* (Lucas, 1846) an early warning indicator species of global warming in the Central Mediterranean Sea. J. Mar. Syst. 138, 29–39. <https://doi.org/10.1016/j.jmarsys.2013.10.007>.

Desforges, J.P.W., Galbraith, M., Ross, P.S., 2015. Ingestion of microplastics by zooplankton in the Northeast Pacific Ocean. Arch. Environ. Contam. Toxicol. 69, 320–330. <https://doi.org/10.1007/s00244-015-0172-5>.

Devriese, L.I., van der Meulen, M.D., Maes, T., Bekaert, K., Paul-Pont, I., Frère, L., Robbans, J., Vethaak, A.D., 2015. Microplastic contamination in brown shrimp (*Crangon crangon*, Linnaeus 1758) from coastal waters of the Southern North Sea and Channel area. Mar. Pollut. Bull. 98, 179–187. <https://doi.org/10.1016/j.marpolbul.2015.06.051>.

Dinno, A., 2024. Dunn's test of multiple comparisons using Rank Sums. R package version 1.3.6. <https://CRAN.R-project.org/package=dunn.test>.

D'Iorio, C., Di Fresco, D., Spanò, N., Albano, M., Panarello, G., Laface, F., Faggio, C., Capillo, G., Savoca, S., 2022. Occurrence of anthropogenic debris in three commercial shrimp species from South-Western Ionian Sea. Biology 11, 1616. <https://doi.org/10.3390/biology1111616>.

Erni-Cassola, G., Zadjelevic, V., Gibson, M.I., Christie-Oleza, J.A., 2019. Distribution of plastic polymer types in the marine environment: a meta-analysis. J. Hazard. Mater. 369, 691–698. <https://doi.org/10.1016/j.jhazmat.2019.02.067>.

Fanelli, E., Cartes, J.E., 2008. Spatio-temporal changes in gut contents and stable isotopes in two deep Mediterranean pandalids: influence on the reproductive cycle. Mar. Ecol. Prog. Ser. 355, 219–233. <https://doi.org/10.3354/meps07260>.

Follesa, M.C., Carbonara, P., 2019. Atlas of the maturity stages of Mediterranean fishery resources. In: Studies and Reviews. General Fisheries Commission for the Mediterranean. No. 99. FAO, Rome.

Fossi, M.C., Pédá, C., Compa, M., Tsangaridis, C., Alomar, C., Claro, F., Ioakeimidis, C., Galgani, F., Hema, T., Deudero, S., Romeo, T., Battaglia, P., Andaloro, F., Caliani, I., Casini, S., Panti, C., Baini, M., 2018. Bioindicators for monitoring marine litter ingestion and its impacts on Mediterranean biodiversity. Environ. Pollut. 237, 1023–1040. <https://doi.org/10.1016/j.envpol.2017.11.019>.

Guijarro, B., Massutí, E., Moranta, J., Cartes, J.E., 2009. Short spatio-temporal variations in the population dynamics and biology of the deep-water rose shrimp *Parapenaeus longirostris* (Decapoda: Crustacea) in the western Mediterranean. Sci. Mar. 73, 183–197. <https://doi.org/10.3989/scimar.2009.73n1183>.

Hartmann, N.B., Hüffer, T., Thompson, R.C., Hassellöv, M., Verschoor, A., Daugaard, A.E., Rist, S., Karlsson, T., Brennholt, N., Cole, M., Herrling, M.P., Hess, M.C., Ivleva, N.P., Lusher, A.L., Wagner, M., 2019. Are we speaking the same language? Recommendations for a definition and categorization framework for plastic debris. Environ. Sci. Technol. 53, 1039–1047. <https://doi.org/10.1021/acs.est.8b05297>.

Hermsen, E., Mintenig, S.M., Besseling, E., Koelmans, A.A., 2018. Quality criteria for the analysis of microplastic in biota samples: a critical review. Environ. Sci. Technol. 52, 10230–10240. <https://doi.org/10.1021/acs.est.8b01611>.

Hidalgo-Ruz, V., Gutow, L., Thompson, R.C., Thiel, M., 2012. Microplastics in the marine environment: a review of the methods used for identification and quantification. Environ. Sci. Technol. 46, 3060–3075. <https://doi.org/10.1021/es2031505>.

Institut Català de Recerca per a la Governança del Mar (ICATMAR), 2021. State of Fisheries in Catalonia 2021, Part 2: Stock Assessment. Barcelona, p. 110. <https://doi.org/10.2436/10.8080.05.15>.

Joyce, H., Nash, R., Kavanagh, F., Power, T., White, J., Frias, J., 2022. Size dependent egestion of polyester fibres in the Dublin Bay prawn (*Nephrops norvegicus*). Mar. Pollut. Bull. 180, 113768. <https://doi.org/10.1016/j.marpolbul.2022.113768>.

Joyce, H., Nash, R., Frias, J., White, J., Cau, A., Carreras-Colom, E., Kavanagh, F.A., 2023. Monitoring microplastic pollution: the potential and limitations of *Nephrops norvegicus*. Ecol. Indic. 154, 110441. <https://doi.org/10.1016/j.ecolind.2023.110441>.

Kapiris, K., 2004. Feeding ecology of *Parapenaeus longirostris* (Lucas, 1846) (Decapoda: Penaeidae) from the Ionian Sea (Central and Eastern Mediterranean Sea). Sci. Mar. 68, 247–256. <https://doi.org/10.3989/scimar.2004.68n2247>.

Kasalica, O., Regner, S., Petrov, B., Joksimović, A., 2011. Some aspects of the reproductive biology of deep-water pink shrimp *Parapenaeus longirostris* (Lucas, 1846) (Decapoda, Penaeidae) on the Montenegrin shelf. Crustaceana 84 (14), 1683–1696. <https://doi.org/10.1163/156854011X608456>.

Ladewig, S.M., Bao, S., Chow, A.T., 2015. Natural fibers: a missing link to chemical pollution dispersion in aquatic environments. Environ. Sci. Technol. 49, 12609–12610. <https://doi.org/10.1021/acs.est.5b04754>.

Lahens, L., Strady, E., Kieu-Le, T.C., Dris, R., Boukerma, K., Rinnert, E., Gasperi, J., Tassin, B., 2018. Macroplastic and microplastic contamination assessment of a tropical river (Saigon River, Vietnam) transversed by a developing megacity. Environ. Pollut. 36, 661–671. <https://doi.org/10.1016/j.envpol.2018.02.005>.

Law, K.L., 2017. Plastics in the marine environment. Ann. Rev. Mar. Sci. 9, 205–229. <https://doi.org/10.1146/annurev-marine-010816-060409>.

Lusher, A., Hernandez-Milian, G., 2018. Microplastic extraction from marine vertebrate digestive tracts, regurgitates and scats: a protocol for researchers from all experience levels. Bio-Protocol 8. <https://doi.org/10.21769/bioprotoc.3087>.

MacLeod, M., Arp, H.P.H., Tekman, M.B., Jahnke, A., 2021. The global threat from plastic pollution. Science 373, 61–65. <https://doi.org/10.1126/science.abg5433>.

Marmara, D., Katsanevakis, S., Brundo, M.V., Tiralongo, F., Ignoto, S., Krasakopoulou, E., 2023. Microplastics ingestion by marine fauna with a particular focus on commercial species: a systematic review. Front. Mar. Sci. 10. <https://doi.org/10.3389/fmars.2023.1240969>.

Menges, F., 2021. J. Spectragraph - Optical Spectroscopy Software. v1.2.16.1 (Version 1.2.16.1) [Software]. <http://www.effemm2.de/spectragraph>.

Milligan, R.J., Albalat, A., Atkinson, R.J.A., Neil, D.M., 2009. The effects of trawling on the physical condition of the norway lobster *Nephrops norvegicus* in relation to seasonal circles in the Clyde Sea area. ICES J. Mar. Sci. 66, 488–494. <https://doi.org/10.1093/icesjms/fsp018>.

Muns-Pujadas, L., Dallarés, S., Constenla, M., Padrós, F., Carreras-Colom, E., Grelaud, M., Carrassón, M., Soler-Membrives, A., 2023. Revealing the capability of the European hake to cope with micro-litter environmental exposure and its inferred potential health impact in the NW Mediterranean Sea. Mar. Environ. Res. 186. <https://doi.org/10.1016/j.marenvres.2023.105921>.

Oksanen, J., Simpson, G., Blanchet, F., Kindt, R., Legendre, P., Minchin, P., O'Hara, R., Solymos, P., Stevens, M., Szeocs, E., Wagner, H., Barbour, M., Bedward, M., Bolker, B., Borcard, D., Carvalho, G., Chirico, M., De Caceres, M., Durand, S., Antoniazi, H.B., FitzJohn, R., Friendly, M., Furneaux, B., Hannigan, G., Hill, M., Lahti, L., McGlinn, D., Ouellette, M.H., Ribeiro, E., Smith, T., Stier, A., Ter, C.J.F., Weedon, J., 2022. vegan: community ecology package. R package version 2.6-4. <http://CRAN.R-project.org/package=vegan>.

Palanques, A., Masqué, P., Puig, P., Sanchez-Cabeza, J.A., Frignani, M., Alvisi, F., 2008. Anthropogenic trace metals in the sedimentary record of the Llobregat continental shelf and adjacent Foix Submarine Canyon (Northwestern Mediterranean). Mar. Geol. 248, 213–227. <https://doi.org/10.1016/j.margeo.2007.11.001>.

Pasterk, S., Ranacher, L., Stern, T., Schuster, K.C., Aigner, D.J., Hesser, F., 2024. How regenerated cellulose fibers appear in the discourse on marine pollution with microplastic: a snowballing and network approach. Environ. Res. Commun. 6 (11), 112001. <https://doi.org/10.1088/2515-7620/ad8ac3>.

R Core Team, 2023. R: A Language and Environment for Statistical Computing. R Foundation for Statistical Computing, v4.2.3 (version 4.2.3) [software]. <https://www.r-project.org>.

Rodríguez-Romeu, O., Constenla, M., Carrassón, M., Campoy-Quiles, M., Soler-Membrives, A., 2020. Are anthropogenic fibers a real problem for red mullets (*Mullus barbatus*) from the NW Mediterranean? Sci. Total Environ. 733. <https://doi.org/10.1016/j.scitotenv.2020.139336>.

Rodríguez-Romeu, O., Constenla, M., Soler-Membrives, A., Dutto, G., Saraux, C., Schull, Q., 2024. Sardines in hot water: unravelling plastic fibre ingestion and

feeding behaviour effects. Environ. Pollut. 363, 125035. <https://doi.org/10.1016/j.envpol.2024.125035>.

Sanchez-Vidal, A., Thompson, R.C., Canals, M., De Haan, W.P., 2018. The imprint of microfibers in southern European deep seas. PLoS One 13, e0207033. <https://doi.org/10.1371/journal.pone.0207033>.

Santini, S., De Beni, E., Martellini, T., Sarti, C., Randazzo, D., Ciraolo, R., Scopetani, C., Cincinelli, A., 2022. Occurrence of natural and synthetic micro-fibers in the Mediterranean Sea: a review. Toxics 10 (7), 391. <https://doi.org/10.3390/toxics10070391>.

Santon Nicola, S., Volgare, M., Coccia, M., Dorigato, G., Giaccone, V., Colavita, G., 2023. Impact of fibrous microplastic pollution on commercial seafood and consumer health: a review. Animals 13 (11), 1736. <https://doi.org/10.3390/ani13111736>.

Sekhon, J.S., 2011. Multivariate and propensity score matching software with automated balance optimization: the Matching package for R. J. Stat. Software 42, 1–52. <https://doi.org/10.18637/jss.v042.i07>.

Sheridan, M., O'Connor, I., Henderson, A.C., 2016. Investigating the effect of molting on gastric mill structure in Norway lobster (*Nephrops norvegicus*) and its potential as a direct ageing tool. J. Exp. Mar. Biol. Ecol. 484, 16–22. <https://doi.org/10.1016/j.jembe.2016.08.005>.

Sobrino, I., Silva, C., Sbrana, M., Kapiris, K., 2005. A review of the biology and fisheries of the deep water rose shrimp, *Parapenaeus longirostris*, in European Atlantic and Mediterranean Waters (Decapoda, Dendrobranchiata, Penaeidae). Crustaceana 78 (10), 1153–1184. <https://doi.org/10.1163/156854005775903564>.

Suaria, G., Achtypi, A., Perold, V., Lee, J.R., Pierucci, A., Bornman, T.G., Aliani, S., Ryan, P.G., 2020. Microfibers in oceanic surface waters: a global characterization. Sci. Adv. 6 (23), 8493. <https://doi.org/10.1126/sciadv.aay8493>.

Tubau, X., Canals, M., Lastras, G., Rayo, X., Rivera, J., Amblas, D., 2015. Marine litter on the floor of deep submarine canyons of the Northwestern Mediterranean Sea: the role of hydrodynamic processes. Prog. Oceanogr. 134, 379–403. <https://doi.org/10.1016/j.pocean.2015.03.013>.

Uddin, S., Fowler, S.W., Uddin, M.F., Behbehani, M., Naji, A., 2021. A review of microplastic distribution in sediment profiles. Mar. Pollut. Bull. 163, 111973. <https://doi.org/10.1016/j.marpolbul.2021.111973>.

Welden, N.A.C., Cowie, P.R., 2016a. Long-term microplastic retention causes reduced body condition in the langoustine, *Nephrops norvegicus*. Environ. Pollut. 218, 895–900. <https://doi.org/10.1016/j.envpol.2016.08.020>.

Welden, N.A.C., Cowie, P.R., 2016b. Environment and gut morphology influence microplastic retention in langoustine, *Nephrops norvegicus*. Environ. Pollut. 214, 859–865. <https://doi.org/10.1016/j.envpol.2016.03.067>.

Woodall, L.C., Robinson, L.F., Rogers, A.D., Narayanaswamy, B.E., Paterson, G.L.J., 2015. Deep-sea litter: a comparison of seamounts, banks and a ridge in the Atlantic and Indian Oceans reveals both environmental and anthropogenic factors impact accumulation and composition. Front. Mar. Sci. 2. <https://doi.org/10.3389/fmars.2015.00003>.

Yücel, N., 2023. Detection of microplastic fibers tangle in deep-water rose shrimp (*Parapenaeus longirostris*, Lucas, 1846) in the Northeastern Mediterranean Sea. Environ. Sci. Pollut. Res. 30, 10914–10924. <https://doi.org/10.1007/s11356-022-22898-w>.